

# Integrated fatigue damage diagnosis and prognosis under uncertainties

Tishun Peng<sup>1</sup>, Jingjing He<sup>1</sup>, Yongming Liu<sup>1</sup>, Abhinav Saxena<sup>2</sup>, Jose Celaya<sup>2</sup>, Kai Goebel<sup>3</sup>

<sup>1</sup>*Department of Civil & Environmental Engineering, Clarkson University, Potsdam, NY, 13699-5725, USA*

*pengt@clarkson.edu*

*jihe@clarkson.edu*

*yliu@clarkson.edu*

<sup>2</sup>*SGT, NASA Ames Research Center, Moffett Field, CA, 94035, USA*

*abhinav.saxena@nasa.gov*

*Jose.r.celaya@nasa.gov*

<sup>3</sup>*NASA Ames Research Center, Moffett Field, CA, 94035, USA*

*kai.goebel@nasa.gov*

## ABSTRACT

An integrated fatigue damage diagnosis and prognosis framework is proposed in this paper. The proposed methodology integrates a Lamb wave-based damage detection technique and a Bayesian updating method for remaining useful life (RUL) prediction. First, a piezoelectric sensor network is used to detect the fatigue crack size near the rivet holes in fuselage lap joints. Advanced signal processing and feature fusion is then used to quantitatively estimate the crack size. Following this, a small time scale model is introduced and used as the mechanism model to predict the crack propagation for a given future loading and an estimate of initial crack length. Next, a Bayesian updating algorithm is implemented incorporating the damage diagnostic result for the fatigue crack growth prediction. Probability distributions of model parameters and final RUL are updated considering various uncertainties in the damage prognosis process. Finally, the proposed methodology is demonstrated using data from fatigue testing of realistic fuselage lap joints and the model predictions are validated using prognostics metrics.

## 1. INTRODUCTION

For aerospace and civil engineering structures, various types of damage such as fatigue cracks, delamination, debonding, and corrosion have significant impact on service life. To reasonably assess their current health condition (Chong 1999; Masri, Sheng et al. 2004), a sensitive and precise

diagnostic method is needed. By analyzing continuous monitoring data, prognostics can provide valuable information for decision making within an effective structural health management (SHM) framework. Fatigue is

the root cause for a variety of failure modes in aircraft and rotorcraft. There are many non-destructive evaluation (NDE) methods available for fatigue damage diagnostics, such as, thermograph (Hung 1996; Koruk 2009), ultrasonics (Kazys and Svilainis 1997), X-ray CT (Nicoletto, Anzelotti et al.), etc. With the development of Lamb wave based damage detection methods, piezoelectric sensors have been widely used (Ward and Buttry 1990; Monkhouse, Wilcox et al. 1997; Lemistre and Balageas 2001; Giurgiutiu, Zagrai et al. 2002; Giurgiutiu 2003; Giurgiutiu 2005; Santoni, Yu et al. 2007) for structural health monitoring because of their low cost and high efficiency (Constantin, Sorohan et al. 2011). Lamb waves can propagate in thin plate without too much dispersion in certain modes (Scalea, Francesco et al. 2002). Using a proper mode selection, piezoelectric sensor networks have also been widely used for damage inspection of composite plate structures (Wang, Rose et al. 2004) and health monitoring of composite lap joints in aircraft wing. The built-in piezoelectric sensors are an ideal way to detect invisible fatigue crack growth in metal structures (Ihn and Chang 2004) and internal delamination in composite beam (JR and Chang 1993). However, most of the existing literatures focus on the plate-like components without more complex geometrical features. Damage is typically investigated away from the specimen boundaries to avoid complex wave reflections. Extending these detection methods to more complex structural components and prognostic enhancements requires further attention.

---

Tishun Peng et al. This is an open-access article distributed under the terms of the Creative Commons Attribution 3.0 United States License, which permits unrestricted use, distribution, and reproduction in any medium, provided the original author and source are credited.

In order to predict fatigue crack propagation, various physics-based models have been developed. Paris' law (Paris and Erdogan 1963) is one of the most acknowledged fracture mechanics-based model for fatigue life prediction. However, Paris's law does not take stress ratio effects into consideration. Several modified versions of Paris' law have been reported in the literature, such as the modification for the near threshold crack growth (Forman 1967; Laird 1979), small/short cracks growth (Kitagawa and Takahashi 1979; Ritchie and Lank 1996), and crack closure (Elber 1970). However, most of these studies employ cycle-based methods and their application to randomly varying spectrums may be difficult. A time-based fatigue crack growth model (Lu and Liu 2010) was suggested that can overcome some of these inherent shortcomings in the classical cycle-based fatigue theories.

Furthermore, fatigue damage accumulation is a stochastic process and an appropriate inclusion and management of various uncertainties is critical for prognostics and decision-making. Bayesian updating algorithm has been shown to make use of condition monitoring data to improve model based prognosis and incorporate effects of different types of uncertainties (Guan, Jha et al. 2011). The uncertainty bounds for life prediction are contained (reduced) by updating the parameter distribution using the detected crack length through periodic measurements. Bayesian updating method has been used in this paper for integrated diagnostics and prognostics under uncertainties for a realistic lap joint geometry.

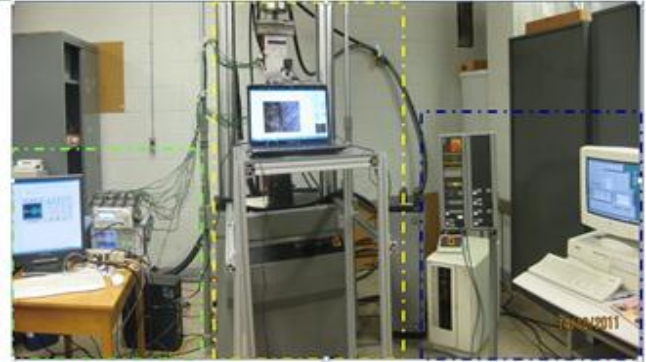
This paper is organized as follows. First, piezoelectric sensor based damage diagnostic method is proposed to detect the crack growth in a lap joint structure. Following this, A Bayes theorem based prognostic method is proposed that makes combined use of the damage detection method and crack propagation models. It is shown that uncertainties involved in the model parameters and detected measurement data are handled through Bayesian updating. Next, experimental data from lap joint coupons are used to demonstrate the applicability of this integrated method followed by model validation through prognostic metrics. The paper ends with conclusions and an outline of future work based on the current effort.

## 2. DAMAGE DIAGNOSIS USING A PIEZOELECTRIC SENSOR NETWORK

### 2.1. Experiment Setup

The experimental setup for damage prognosis of riveted lap joint coupons consists of three major modules: sensing and data acquisition system, fatigue crack ground truth measurement system, and fatigue cycling system (Fig. 1). Sensing and data acquisition system generates a 3.5 cycles tone burst lamb wave from Piezoelectric (PZT) actuators and records the corresponding signal received by PZT

sensors. Crack measurement system uses a traveling microscope to measure the crack length after a certain number of loading cycles at regular intervals. The specimen is subjected to tensile cyclic loading using the fatigue cycling system. The experiment setup is shown in Fig. 1. The coupons were subjected to two types of loading spectrums; constant block loading and variable block loading as shown in Fig. 2.



Sensing and data acquisition system      Fatigue crack ground truth measurement system      Fatigue cycling system

Figure 1. Systematic flow chart for the damage diagnosis system for lap joint

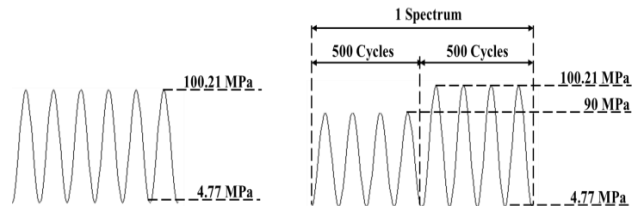


Figure 2. Loading spectrum. a), Constant loading. b), Variable loading

### 2.2. Specimen Geometry and Sensor Layout Design

The riveted panels are made of 0.063 inch Al 2024-T3 sheets that were originally provided by NRC, Canada. For repeatability, additional coupons were manufactured at NASA. Three rows of rivets are embedded in the panels. The detailed geometry is shown in Fig. 3 and corresponding mechanical properties of the material are shown in Table 1. To employ a pitch-catch method (Raghavan and Cesnik 2007), PZTs acting as actuators and sensors are glued on the two sides of the rivet holes.

The experimental results have shown that the major crack, which results in the final failure of the specimen, always appears at the countersunk hole in the first row. Therefore, the first row is considered as the target region for damage detection. In this study, our efforts are focused on detecting damage in the target region and accordingly, the actuators and the sensors are placed on opposite sides of the first row. This ensures the crack would be on the direct wave path of

the sensor-actuator pairs whenever it appears. The corresponding sensor network configuration is shown in Fig. 4. Red dots represent actuators away from the target region and the green dots represent sensors near the target region. Each pair of sensors can interrogate the damage information on their direct wave path.

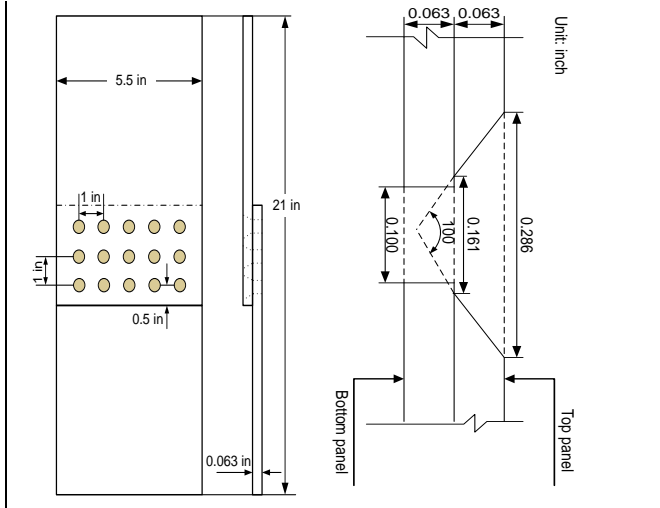


Figure 3. Geometry of the lap joint and detailed dimension of the connection part

Material	Yield strength (Mpa)	Modulus of elasticity (Mpa)	$\sigma_u$ (Mpa)	$\Delta K_{th}$ (Mpa $m^{0.5}$ )
Al2024-T3	360	72000	490	1.1164

Table 1. Mechanical properties of Al2024-T3

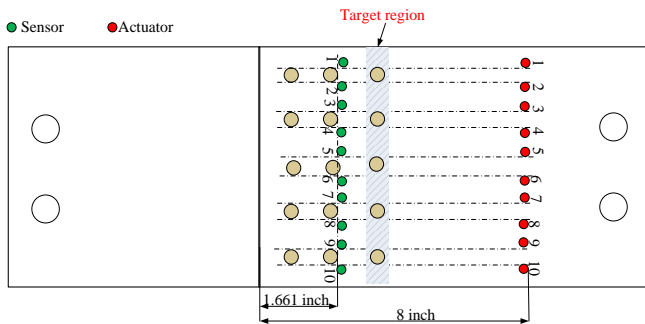


Figure 4. Sensor network layout for damage detection on riveted lap joint

### 2.3. Experimental Result and Data Processing

In this study, a Hamming-windowed sinusoidal tone burst with 3.5 cycles was used as the actuating signal. The central frequency of this signal was set at 200kHz, as shown in Fig. 5. After installing the specimen on the hydraulic machine, first a baseline signal for normal condition is collected.

Further data are collected periodically and the traveling microscope is used to measure the surface crack length at regular intervals. Fig. 6 illustrates a typical signal obtained for specimen T11 subjected to constant loading. With further signal processing, changes in selected features (phase change, correlation coefficient, and amplitude change) are calculated. The amplitude change reflects the energy dissipation due to the crack. The phase angle change is due to the traveling distance change due to the crack. The correlation coefficient change reflects the signal perturbation due to the new waves generated at the crack surfaces (Raghavan and Cesnik 2007). The detailed physical explanation of the chosen features is discussed in a companion papers and is under preparation. All of these feature changes can be obtained by comparing the received signals under normal and defect condition. Detailed description is given in literatures (Zhao, Gao et al. 2007; SU and Ye 2009; Wang and Yuan 2009). The relationship between trends in features and crack length is shown in Fig. 7.

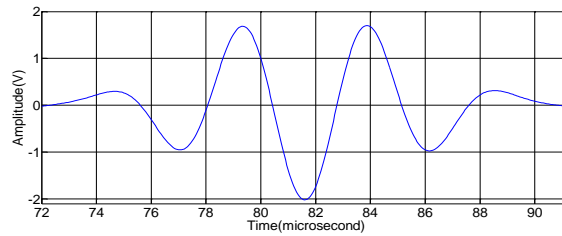


Figure 5. A tone burst signal of 3.5 cycles with 200kHz central frequency

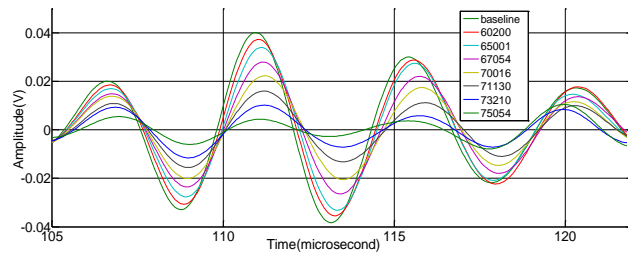


Figure 6. Received signal for specimen T11

Cycle#	Correlation coefficient	Phase change	Amplitude
55900	1	0	0.0201
60200	0.9895	0	0.0185
65001	0.9777	0.05	0.017
67054	0.9481	0.1	0.0149
70016	0.9233	0.1	0.0139
71130	0.9058	0.15	0.0109
73210	0.8717	0.15	0.0093
75045	0.7762	0.3	0.0055

Table 2. The corresponding signal interpreting result for T11 under constant loading

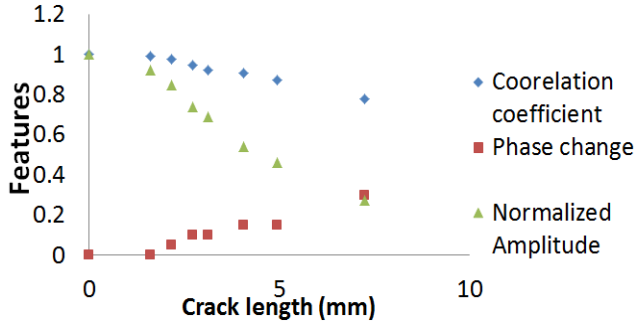


Figure 7. The relationship between signal features and crack length

As shown in Table 2. and Fig. 7, all features exhibit monotonic relationships with increasing crack length, but it is not trivial to predict the crack length using individual feature. Therefore, using data from several experiments, a multivariable regression is carried out. The corresponding formulation is shown in Eq. (1), which is trained using data from five different specimens (T1, T2, T3, T5 and T6). Table 2 lists the tuned regression coefficients for this formulation.

$$a = A + \alpha_1x + \alpha_2y + \alpha_3z + \alpha_4xy + \alpha_5xz + \alpha_6yz + \alpha_7x^2 + \alpha_8y^2 + \alpha_9z^2 \quad (1)$$

where  $A$  is the detected crack length,  $x$  is the correlation coefficient variable,  $y$  is the phase change variable, and  $z$  is the amplitude variable.

Coefficients	Value
$A$	7.92
$\alpha_1$	-2.77
$\alpha_2$	-2.69
$\alpha_3$	-9.41
$\alpha_4$	0.529
$\alpha_5$	-5.19
$\alpha_6$	10.0
$\alpha_7$	6.21
$\alpha_8$	0.670
$\alpha_9$	3.50

Table 4. Coefficients for second order multivariate regression

Using the diagnostic model described above, detected crack length for various specimen can be obtained. Table 3. shows experimentally measured crack lengths and the detection results for the two specimens (T11 and T9). It can be observed that detection results show good agreement with ground truth crack length measurements in general. However, there are uncertainties in these measurements and diagnostic estimation which show up as differences in the two estimates. A similar behavior was observed for all other specimens. .

T11 Constant loading		T9 Variable loading	
Measured Crack length(mm)	Detected Crack length(mm)	Measured Crack length(mm)	Detected Crack length(mm)
0	0.257	0	0.257
1.61	0.834	1.94	2.77
2.17	1.71	2.5	3.01
2.74	2.71	3.71	3.79
3.13	2.99	3.88	4.40
4.06	4.38	4.61	4.79
4.96	4.90	4.96	4.75
7.24	6.30	5.52	5.01

Table 3. The experimentally measured crack length and detected result for the two specimens

### 3. DAMAGE PROGNOSIS USING BAYESIAN UPDATING

Following the development of the damage diagnosis model, the detected crack growth data are combined with crack propagation law for the predicting remaining life. A small time scale model (Lu 2010) is briefly discussed next, which was used as the mechanism model for fatigue crack propagation. Bayes theorem based prognostic method is then employed to incorporate diagnostic estimation and fatigue crack growth model.

#### 3.1. Small Time Scale Model

This model defines the fatigue crack kinetics at any arbitrary time instant ( $t+dt$ ) within a loading cycle. As shown in Fig. 8, the crack face will extend by  $da$  for a small temporal increment  $dt$  during the loading cycle (Lu and Liu 2010). The crack growth after a given life span ( $\Delta t$ ) can be obtained through direct integration over time. This model was proposed based on the geometric relationship between the crack tip opening displacement (CTOD) and the instantaneous crack growth kinetics. An illustration of this geometric relationship is shown in Fig. 9. For a given time increment, the relationship between the CTOD increment  $d\delta$  and crack increment  $da$  can be expressed as

$$\frac{da}{dt} = \frac{ctg\theta}{2} \frac{d\delta}{dt} \quad (2)$$

where  $\theta$  is the crack tip opening angle (CTOA). However, this formulation does not consider material property changes at the crack tip during previous loading cycles. To incorporate that, the relationship between  $da$  and  $d\delta$  was modified by (Zhang and Liu 2012). This model is also

applicable to random amplitude loading in general and is given as

$$\frac{da}{dt} = \frac{AK_{\max}\Delta K d\delta}{2\sqrt{\delta} dt} \quad (3)$$

where  $A$  is a calibration parameter for a given specimen,  $\Delta K = \Delta\sigma\sqrt{\pi a}Y$  and  $Y$  is the geometry correction function. A detailed derivation of this formulation can be found in (Lu and Liu 2010).

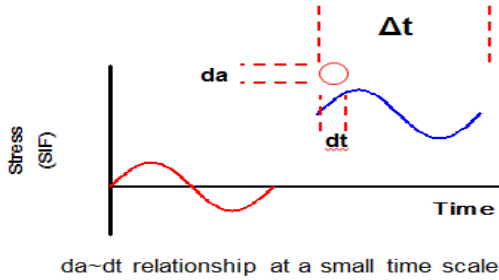


Figure 8. da-dt relationship at a small time scale

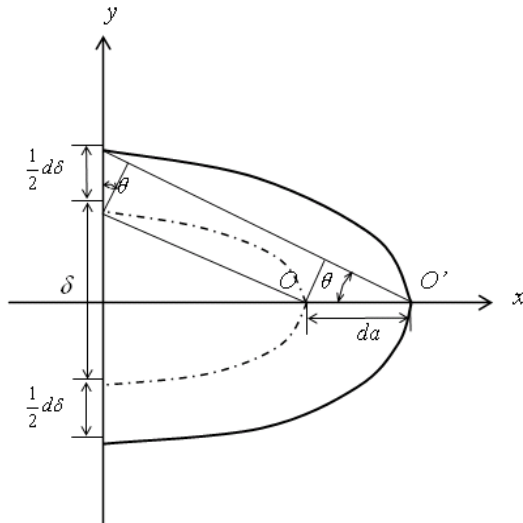


Figure 9. A schematic illustration of the geometric relationship for crack tip

### 3.2. Bayesian updating and uncertainties quantification

Even though the introduced small time scale model can express the fatigue crack growth under variable amplitude loading, this deterministic model cannot handle the uncertainties involved in the fatigue crack growth. Maximum Relative Entropy (MRE) was first applied by (Guan, Jha et al. 2009) in fatigue problems to describe the stochastic process of the fatigue crack growth mechanism. Model parameters are considered as random variables, which can be updated using the in-situ measurements. The posterior distribution of the parameters can be expressed as

$$q(\theta) \propto p(\theta)p(x|\theta)\exp(\beta g(\theta)) \quad (4)$$

where  $p(\theta)$  is the prior distribution of the model parameter, in which  $\theta$  can be vector,  $p(x|\theta)$  is the likelihood function,  $q(\theta)$  is the posterior distribution of model parameter,  $\exp(\beta g(\theta))$  is the term introduced by the moment constraint. The detailed derivation of Eq.(4) can be found in al(Guan, Jha et al. 2009). It can be seen that, if there is no moment constraint (i.e.,  $\beta = 0$ ), MRE method is identical with traditional Bayesian updating. In Bayesian updating, model uncertainties and measurements uncertainties are incorporated in the construction of the likelihood function. Let  $x'$  be a system measurement,  $M(\theta)$  is the prediction value based on physic-model. If there is no measurement noise and model parameter uncertainties, the measurement would be identical with the model prediction, i.e.  $x' = M(\theta)$ . However, this is not the case here. If the measurement noise  $\epsilon$  and model uncertainties  $\tau$  are considered, the relationship between  $x'$  and  $M(\theta)$  can be expressed as

$$x' = M(\theta) + \epsilon + \tau \quad (5)$$

Assume the two error term  $\epsilon$  and  $\tau$  are independent zero mean normal variables (Bell 2001; Adams 2002), the sum of them can be expressed as a new random variable  $e = (\epsilon + \tau) \sim N(0, \sigma_e)$ . Therefore, the likelihood function  $p(x'|\theta)$  can be expressed as

$$p(x'_1, x'_2, \dots, x'_n | \theta) = \frac{1}{(\sqrt{2\pi}\sigma_e)^n} \exp\left(-\frac{1}{2}\sum_{i=1}^n \left(\frac{x'_i - M(\theta)}{\sigma_e}\right)^2\right) \quad (6)$$

Where  $n$  is the number of available measurements. Substituting Eq.(6) into Eq.(4), the posterior distribution of parameter  $\theta$  is expressed as

$$p(\theta|x'_1, x'_2, \dots, x'_n) \propto p(\theta) \frac{1}{(\sqrt{2\pi}\sigma_e)^n} \exp\left(-\frac{1}{2}\sum_{i=1}^n \left(\frac{x'_i - M(\theta)}{\sigma_e}\right)^2\right) \quad (7)$$

In Eq. (7),  $M(\theta)$  can be replaced by the small time scale model introduced earlier. The crack length can be calculated using given parameter inputs. It is not easy to get an analytical solution for Eq. (7) if the parameter vector is high dimension. Therefore, a sample technique, such as Markov chain Monte Carlo (MCMC) is adopted. Following the Bayesian updating, the uncertainties in model parameters are reduced and result in improved remaining useful life prediction performance.

## 4. DEMONSTRATION EXAMPLES

### 4.1. Constant Loading Case

To precisely predict the fatigue life, an estimate of initial crack length is needed as input to the crack growth model. However, the initial crack length for the lap joint is often undetectable initially and therefore an equivalent initial flaw size (EIFS) concept (Liu and Mahadevan 2009) is applied to calculate the crack length for a given number of load cycles.

Ideally EIFS should be properly chosen to match as close as possible the true crack growth area. We consider both EIFS and A in Eq. (3) as the parameters to be updated. The initial guess about A is obtained from training data from other specimens (T1, T2, T3, T5 and T6 ) and the initial estimate of EIFS is obtained by the model proposed in (El, Topper et al. 1979). The equation estimating the EIFS is given as

$$a = \frac{1}{\pi} \left( \frac{\Delta K_{th}}{\Delta \sigma_f Y} \right)^2 \quad (8)$$

where Y is a geometry correction factor depending on specimen geometry and crack configuration,  $\Delta \sigma_f$  is fatigue limit, and  $\Delta K_{th}$  is the threshold stress intensity factor. For lap joints, Y should incorporate the multiple crack condition, because of other minor cracks that may appear randomly near other holes. Corresponding detailed solution for Y is given in (hijazi, Smith et al. 2004).

Based on the prognostic method described above and detected crack length from the diagnosis module in Table 3, Bayesian updating is performed to update the prediction results and the model parameters. The experimentally measured crack length is considered as ground truth data. Fig. 10 shows the prior belief and two set of data and Fig. 11 shows the updated results from the proposed prognosis method. Blue solid line is the median prediction using the prior distribution. Hollow rectangular points are the optically measured crack length and are considered the true crack length. Black solid points are the crack estimation from the Lamb wave-based damage detection method. It can be seen that measurement uncertainties exist and influence the estimated crack length, which is different from the true crack length.

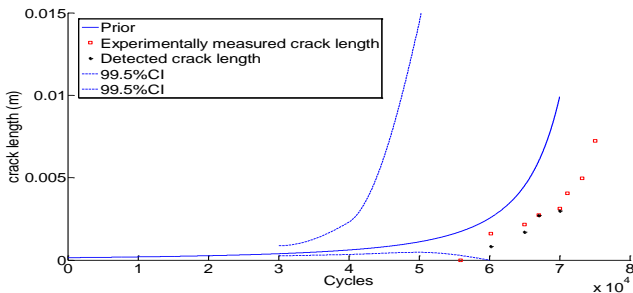
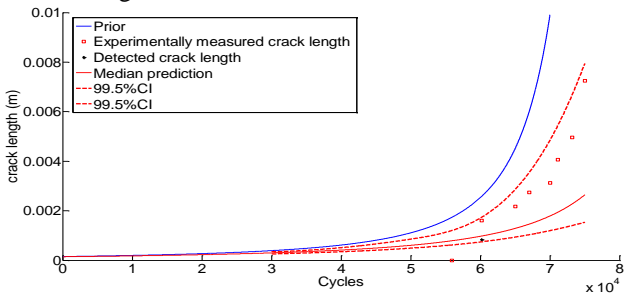
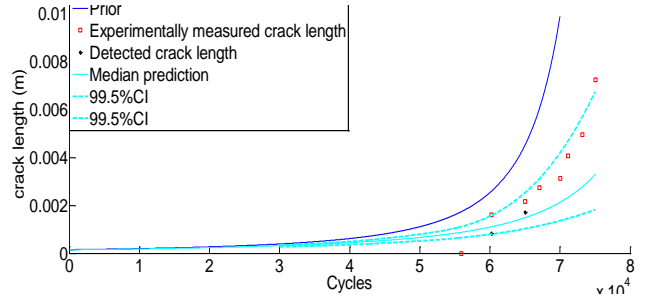


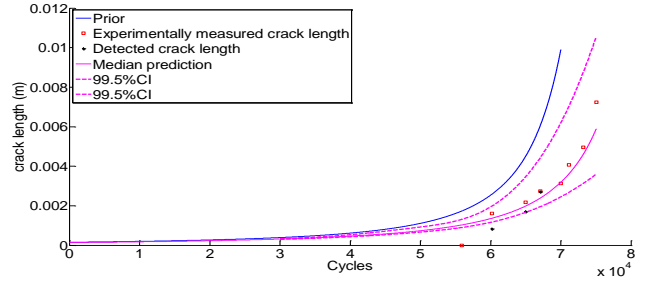
Figure 10. Prior belief and dataset for T11



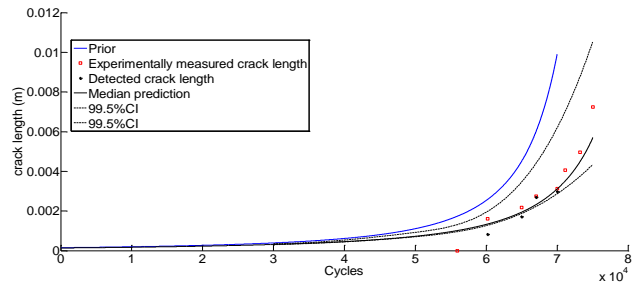
a.



b.



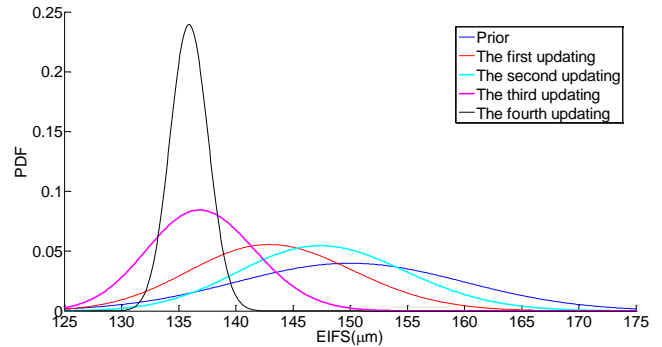
c.



d.

Figure 11. Bayesian updating result. a), One detected data. b), Two detected data. c), Three detected data. d), Four detected data.

From Fig. 11, it can also be seen that the median prediction gets closer to the true crack length with incremental updates from detection data. The uncertainty bounds become narrower with additional updating, which indicate the effectiveness of the Bayesian updating method in reducing prognostic uncertainties. This trend can also be observed in the updated parameter distribution, shown in Fig. 12.



a.

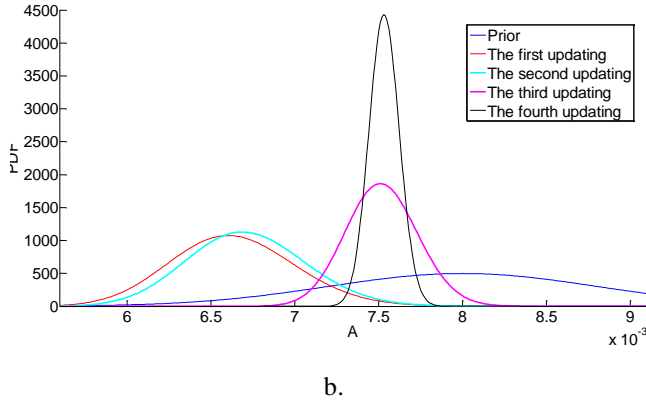


Figure 12. Parameter updating result. a), Updated EIFS. b), Updated A

### 4.2. Variable Loading Case

Following the same procedure as described in Section 4.1, the prognosis is carried out for variable amplitude loading. Fig. 13 shows the prior belief and two sets of data (i.e., crack length measurement from optical microscope and those from Lamb wave detection). Fig. 14 shows the updated results using the proposed prognosis method.

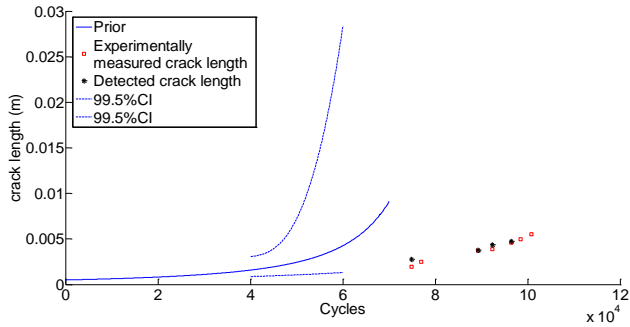


Figure 13. Prior belief and dataset for T9

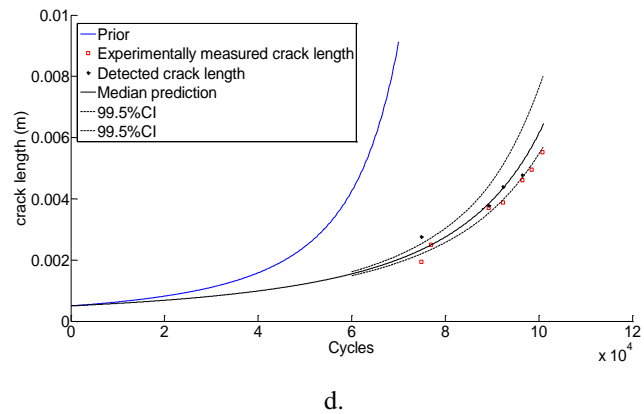
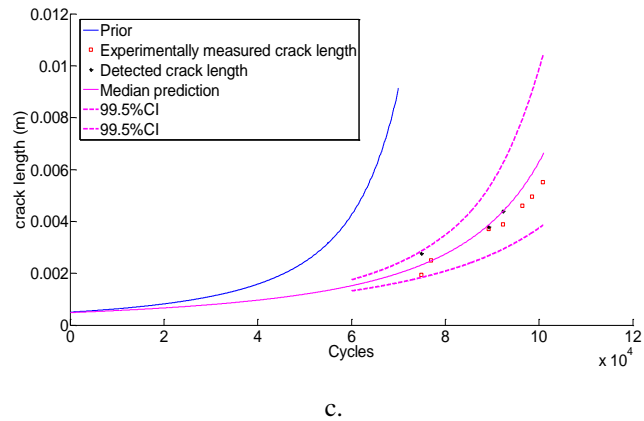
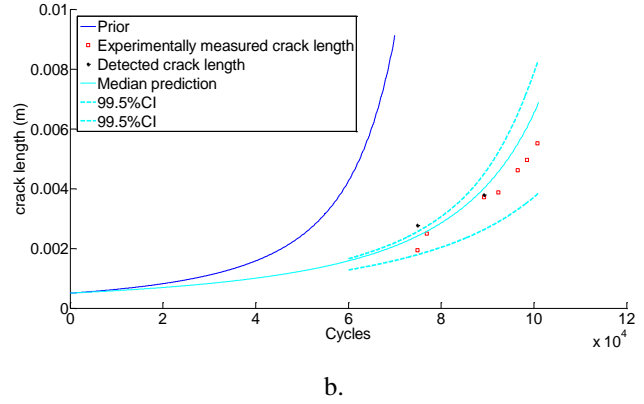
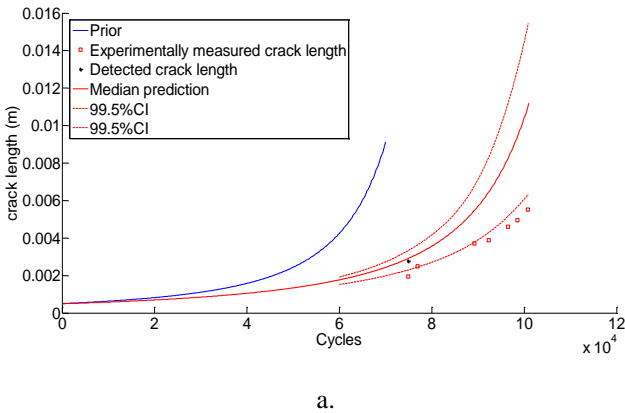
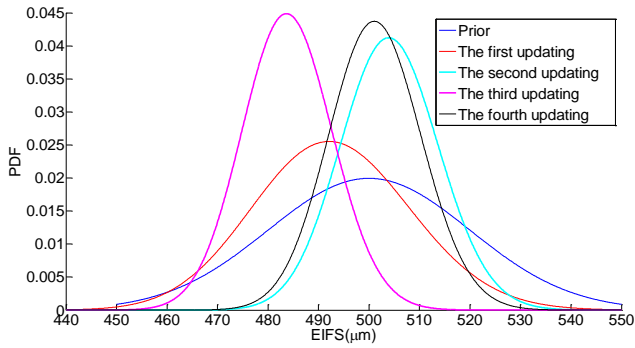


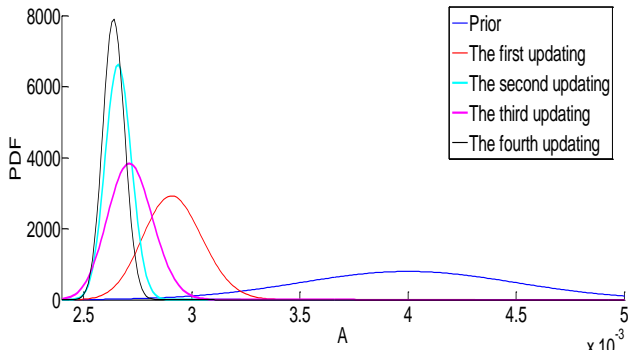
Figure 14. Bayesian updating results with. a), One detected data point. b), Two detected data points. c), Three detected data points. d), Four detected data points.

From the figure above, a similar trend can be observed for the updated crack growth trajectory as well as for the constant amplitude loading case. Fig. 15 shows the updated parameter distribution. In Fig. 15a, the shift between the third and fourth updating is because of the uncertainty of the detected crack size, i.e. measurement error. A further shift is possible for the fifth updating, but the uncertainty of updated parameter distribution won't change too much. The shift is also important as it represents the mean prediction. The tightening of curves reflects the uncertainty decrease. It

is possible to move from inside of 90% to outside of 90% due to the variable loading.



a.



b.

Figure 15. Parameter updating result. a), Updated EIFS. b), updated A

### 4.3. Prognostic Performance Evaluation

To evaluate the performance of the prognostic model, prognostic metrics are employed. A detailed discussion of metrics-based model validation can be found in (Saxena, Celaya et al. 2008). Several relevant metrics, such as Prognostic Horizon (PH),  $\alpha - \lambda$  Accuracy, Relative Accuracy (RA), Cumulative Relative Accuracy (CRA), and Convergence are discussed in that publication. In this paper here, Prognostic Horizon and  $\alpha - \lambda$  Accuracy are used to assess prognostic algorithms performance. The Prognostic Horizon describes the length of time before end-of-life (EoL) when a prognostic algorithm starts predicting with desired accuracy limits. The limit is expressed using an  $\alpha$ -bound given by  $\pm \alpha \cdot t_{EoF}$ . In contrast,  $\alpha - \lambda$  Accuracy determines whether prediction accuracy is within desired accuracy levels (specified by  $\alpha$ ) at a given time. We present the results for constant loading and variable loading in the next figures.

- Constant loading prediction performance assessment

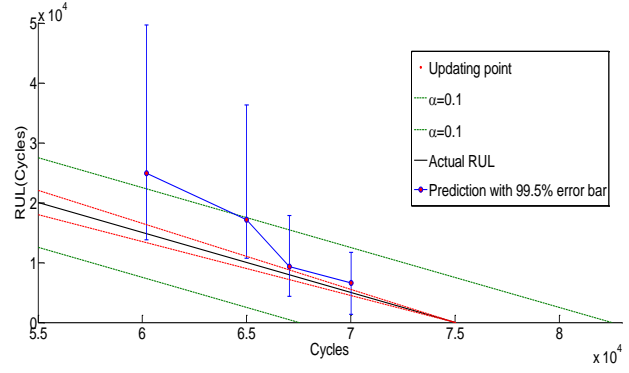


Figure 16. Prognostic performance for PH and  $\alpha - \lambda$  accuracy

Fig. 16 shows that 99.5% RUL interval prediction enters the 90% accuracy zone at the third updating, so the proposed prognostic method can provide a satisfactory prediction of RUL.

- Variable loading prognostic assessment

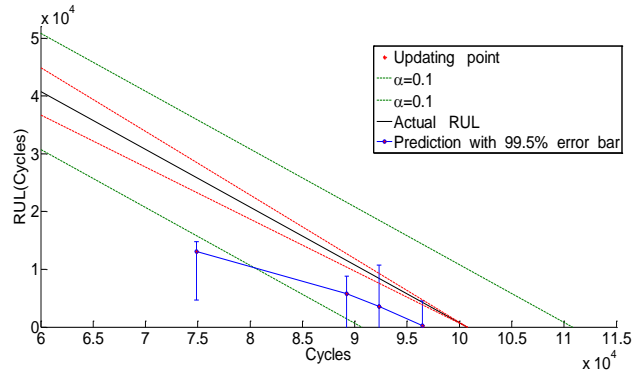


Figure 17. Prognostic performance for PH and  $\alpha - \lambda$  accuracy

From Fig. 17, the same trend can be observed. The 99.5% RUL interval prediction enters the 90% accuracy zone at the fourth updating. Satisfactory result is obtained for the variable loading case.

With additional updating, the median prediction gets closer to the true RUL and the confidence bound is reduced as given more information. Therefore, the updating result can provide an informative RUL prediction at earlier stage of the whole lifecycle.

### 5. CONCLUSION

In this paper, an integrated fatigue damage diagnostics and prognostics methodology is proposed, which combines a piezoelectric sensor network-based damage detection method, physics-based fatigue crack propagation model, and a Bayesian updating framework. The proposed method is demonstrated and validated using fuselage lap joints test



data. Based on the results obtained, several conclusions can be drawn:

1. Individual feature is not adequate for accurate extrapolation from training data to validation data and therefore, feature fusion among different features can be used to reduce the uncertainties in the damage detection;
2. By properly interpreting the features changes of the received signal, the proposed diagnostic model provides a reasonable estimate of the crack length in lap joints. There is some uncertainties inherent in the crack length detection that must be incorporated in predictions.
3. The small time scale model can be successfully applied to both constant loading and variable amplitude loading cases.
4. Bayesian updating can represent and manage the uncertainties introduced by model parameters and measurement noise. The accuracy of model prediction increases as more data are included in the updating. The performance of the proposed prognostic method is assessed by the given prognostics metrics and satisfactory results are obtained.

The current work focused on the damage size estimation for a known damage location identified based on hot spot identification (and consequent sensor placement). Further efforts are required to provide capability for more general crack location methods and to extend the proposed methodology to other structural components. Last but not the least, this work assumed presence of a single major crack for predictions. Further studies are required to consider multiple site cracks and their interactions.

#### ACKNOWLEDGEMENT

The research reported in this paper was supported by the NASA ARMD/AvSP IVHM and SSAT projects under NRANX09AY54A. The support is gratefully acknowledged.

The authors also thank the in-kind support for testing specimens and technical discussions with Dr. Min Liao at NRC Canada and Mr. Mike Venti of NASA Dryden Flight Research Center for providing and manufacturing additional test specimen.

#### REFERENCES

Adams, M. Thomas (2002) "G104-A2L Guide for estimation of measurement uncertainty in testing" American Association of Laboratory Accreditation Manual: 10-18.

Bell, Stephanie (2001) "A Beginner's Guide to Uncertainty of Measurement" The National Physical Laboratory (2): 9-16.

Chong, K. P. (1999). "Health monitoring of Civil structures " *J. Intell. Mater. Syst. Struct* 9(11): 892-898.

Constantin, N., S. Sorohan, et al. (2011). "Efficient and low cost PZT network for detection and localization of damage in low curvature panels." *Journal of Theoretical and Applied Mechanics* 49(3): 685-704.

El, H. M., T. Topper, et al. (1979). "Prediction of nonpropagating cracks." *Eng. Fract. Mech.* 11: 573-584.

Elber, W. (1970). "Fatigue crack closure under cyclic tension." *Eng. Fract. Mech.* 21: 37-45.

Forman, R. (1967). "Numerical analysis of crack propagation in cyclic-loaded structures." *J Basic Eng* 89: 459-464.

Giurgiutiu, V. (2003). "Lamb wave generation with piezoelectric wafer active sensors for structural health monitoring." *Smart Structures and Materials* 5056: 111-122.

Giurgiutiu, V. (2005). "Tuned Lamb wave excitation and detection with piezoelectric wafer active sensors for structural health monitoring." *Journal of Intelligent Material Systems and Structures* 16(4): 291.

Giurgiutiu, V., A. Zagari, et al. (2002). "Piezoelectric wafer embedded active sensors for aging aircraft structural health monitoring." *Structural Health Monitoring* 1(1): 41-61.

Guan, X., R. Jha, et al. (2009). "Probabilistic fatigue damage prognosis using maximum entropy approach." *Journal of Intelligent Manufacturing*: 1-9.

Guan, X., R. Jha, et al. (2011). "Model Selection, Updating and Averaging for Probabilistic Fatigue Damage Prognosis." *Structural Safety* 33(3): 242-249.

hijazi, A. L., B. L. Smith, et al. (2004). "Linkup strength of 2024-T3 bolted lap joint panels with multiple-site damage." *Journal of Aircraft* 41(2): 359-364.

Ihn, J.-B. and F.-K. Chang (2004). "Detection and monitoring of hidden fatigue crack growth using a built-in piezoelectric sensor/actuator network: I. Diagnostics." *Smart Mater. Struct.* 13: 609-620.

JR, C. H. K. and F.-K. Chang (1993). " Identifying delamination in composite beams using built-in piezoelectrics." *J. Intell. Mater. Syst. Struct* 6: 649-672.

Kazys, R. and L. Svilainis (1997). "Ultrasonic detection and characterization of delaminations in thin composite plates using signal processing technique." *Ultrasonics* 35: 367-383.

Kitagawa, H. and S. Takahashi (1979). "Applicability of fracture mechanics to very small cracks or cracks in the early stage.ASM." In: *Proceedings of the second international conference on mechanical behaviour of materials*: 627-631.

Koruk, M., & Kilic, M. (2009). "The usage of IR thermography for the temperature measurements inside an automobile cabin." *International Communication in Heat and Mass Transfer* 36(872-877).

- Laird, C. (1979). "Mechanisms and theories of fatigue." *Fatigue Microstruct.*: 149-203.
- Lemistre, M. and D. Balageas (2001). "Structural health monitoring system based on diffracted Lamb wave analysis by multiresolution processing." *Smart materials and structures* 10: 504.
- Liu, Y. and S. Mahadevan (2009). "Probabilistic fatigue life prediction using an equivalent initial flaw size distribution." *International Journal of Fatigue* 31(3): 476-687.
- Lu, Z. and Y. Liu (2010). "Small time scale fatigue crack growth analysis." *International Journal of Fatigue* 32(8): 1306-1321.
- Masri, S. F., L. H. Sheng, et al. (2004). "Application of a web-enabled real-time structural health monitoring system for civil infrastructure systems." *Smart MATER. STRUCT.* 13(6): 1269-1283.
- Monkhouse, R., P. Wilcox, et al. (1997). "Flexible interdigital PVDF transducers for the generation of Lamb waves in structures." *Ultrasonics* 35(7): 489-498.
- Nicoletto, G., G. Anzelotti, et al. "X-ray computed tomography vs. metallography for pore sizing and fatigue of cast Al-alloys." *Pocedia Engineering* 2: 547-554.
- Paris, P. and F. Erdogan (1963). "A critical analysis of crack propagation laws." *Journal of Basic Engineering, Transactions of the American Society of Mechanical Engineers*: 528-534.
- Raghavan, A. and C. E. S. Cesnik (2007). "Review of guided-wave structural health monitoring." *Shock and Vibration Digest* 39(2): 91-116.
- Ritchie, R. and J. Lank (1996). "Small fatigue cracks: a tatement of the problem and potential solutions." *Mater. Sci. Eng.* 84: 11-16.
- Santoni, G. B., L. Yu, et al. (2007). "Lamb wave-mode tuning of piezoelectric wafer active sensors for structural health monitoring." *Journal of Vibration and Acoustics* 129: 752.
- Saxena, A., J. Celaya, et al. (2008). "Metrics for evaluating performance of prognostic techniques." In *Aerospace conference, 2009 IEEE*: 1-13.
- Scalea, d., L. Francesco, et al. (2002). "Guided wave ultrasonics for NDE of aging aircraft components " *Proc. SPIE* 4704: 123-132.
- SU, Z. and L. Ye (2009). "Identification of damage using Lamb waves." *Springer LNACM* 48: 195-254.
- Wang, C. H., J. T. Rose, et al. (2004). "A synthetic time-reversal imaging method for structural health monitoring." *J. of smart mater. Struct.* 13: 413-423.
- Wang, Q. and S. Yuan (2009). "Baeline-free imaging method based on new pzt sensor arrangements." *Journal of Intelligent Material Systems and Structures* 20(1663-1673).
- Ward, M. D. and D. A. Buttry (1990). "In situ interfacial mass detection with piezoelectric transducers." *Science* 249(4972): 1000.
- Zhang, W. and Y. Liu (2012). "Investigation of incremental fatigue crack growth mechanisms using in situ SEM testing." *Internatinal Journal of Fatigue* 42: 14-23.
- Zhao, X., H. Gao, et al. (2007). "Active health monitoring of an aircraft wing with embedded piezoelectric sensor/actuator network.I.Defect detection, localization and growth monitoring " *Smart MATER. STRUCT.* 16(1208-17).

## BIOGRAPHIES

**Tishun Peng** is a Ph.D. student in the department of civil & environmental engineering at Clarkson University. He received his Bachelor's degree in civil and environmental engineering at Harbin Institute of Technology, China in 2011. His research interests are Bayesian updating and applications, structure diagnostic and probability prognostic, Markov Chain Monte Carlo simulation and reliability.

**Jingjing He** is a graduate research assistant in the department of civil and environmental engineering at Clarkson University. Her research interests are fatigue analysis, structural dynamics, diagnosis and prognosis. She received her B.S. degree in reliability engineering and M.S. degree in aerospace system engineering from Beihang University in China in 2005 and 2008, respectively.

**Yongming Liu** is an associate Professor in the department of civil & environmental engineering. He completed his Bachelors` and Maters` degrees from Tongji University in China and obtained his Ph.D. at Vanderbilt University. His research interests include fatigue and fracture analysis of metals and composite materials, probabilistic methods, computational mechanics, and risk management. Dr. Liu is a member of ASCE and AIAA and serves on several technical committees on probabilistic methods and advanced materials.

**Abhinav Saxena** is a Research Scientist with Stinger Ghaffarian Technologies at the Prognostics Center of Excellence NASA Ames Research Center, Moffet Field CA. His research focus lies in developing and evaluating prognostic algorithms for engineering systems using soft computing techniques. He is a PhD in Electrical and Computer Engineering from Georgia Institute of Technology, Atlanta. He earned his B. Tech in 2001 from Indian Institute of Technology (IIT) Delhi, and Masters` Degree in 2003 from Georgia Tech. Abhinav has been a GM manufacturing scholar and is also a member of IEEE, AAAI and ASME.

**Jose R. Celaya** is a staff scientist with Stinger Ghaffarian Technologies at the Prognostics Center of Excellence, NASA Ames Research Center. He received a Ph.D. degree in Decision Sciences and Engineering Systems in 2008, a

M. E. degree in Operations Research and Statistics in 2008, a M. S. degree in Electrical Engineering in 2003, all from Rensselaer Polytechnic Institute, Troy New York; and a B.S. in Cybernetics Engineering in 2001 from CETYS University, Mexico.

**Kai Goebel** received the degree of Diplom-Ingenieur from the Technische University Munchen, Germany in 1990. He received the M.S. and Ph.D. from the University of California at Berkeley in 1993 and 1996, respectively. Dr. Goebel is a senior scientist at NASA Ames Research Center where he is the deputy area lead for Discovery and Systems Health in the Intelligent Systems division. In addition, he directs the Prognostics Center of Excellence and he is the Associate Principal Investigator for Prognostics of NASA's Integrated Vehicle Health Management Program. He worked at General Electric's Corporate Research Center in Niskayuna, NY from 1997 to 2006 as a senior research scientist. He has carried out applied research in the areas of artificial intelligence, soft computing, and information fusion. His research interest lies in advancing these techniques for real time monitoring, diagnostics, and prognostics. He holds fifteen patents and has published more than 200 papers in the area of systems health management.